Geomechanics and Engineering, *Vol. 23, No. 1 (2020) 71-83*
DOI: https://doi.org/10.12989/gae.2020.23.1.071

Lateral earth pressure and bending moment on sheet pile walls due to uniform surcharge

Akshay Pratap Singh[a] and Kaustav Chatterjee*

Department of Civil Engineering, Indian Institute of Technology Roorkee, Roorkee 247 667, India

(Received January 15, 2020, Revised August 15, 2020, Accepted September 10, 2020)

Abstract. Cantilever sheet pile walls are subjected to surcharge loading located on the backfill soil and at different distances from the top of the wall. The response of cantilever sheet pile walls to surcharge loadings at varying distances under seismic conditions is scarce in literature. In the present study, the influence of uniform surcharge load on cantilever sheet pile wall at varying distances from the top of the wall under seismic conditions are analyzed using finite difference based computer program. The results of the numerical analysis are presented in non-dimensional form like variation of bending moment and horizontal earth pressure along the depth of the sheet pile walls. The numerical analysis has been conducted at different magnitudes of horizontal seismic acceleration coefficient and vertical seismic acceleration coefficients by varying the magnitude and position of uniform surcharge from the top of the wall for different embedded depths and types of soil. The parametric study is conducted with different embedded depth of sheet pile walls, magnitude of surcharge on the top of the wall and at a distance from the top of the wall for different angles of internal friction. It is observed that the maximum bending moment increases and more mobilization of earth pressure takes place with increase in horizontal seismic acceleration coefficients, magnitude of uniform surcharge, embedded depth and decrease in the distance of surcharge from the top of the wall in loose sand.

Keywords: seismic; surcharge; finite difference; sheet pile; embedded depth

1. Introduction

Cantilever sheet pile walls are generally used for temporary as well as permanent structures to hold a limited height (less than 5m) of soil. The holding height is limited because cantilever sheet pile wall derives its stability mainly from the contact stresses developed below the dredge level along the embedded depth of the wall. Cantilever sheet pile walls have been analyzed under static and seismic conditions by various researchers (King 1995, Madabhushi and Chandrasekaran 2005, Madabhushi and Zeng 2006, Callisto and Soccodato 2010, Bowles 2012, Conti *et al.* 2012, Conti and Viggiani 2013, Callisto 2014, Conti *et al.* 2014, Conte *et al.* 2017, Singh and Chatterjee 2020a, b). However, the previous researchers have designed cantilever sheet pile walls using limit equilibrium approach and by assuming the rigid rotation about a pivot point near the toe of the wall due to its simplicity (Conti *et al.* 2013, Conte *et al.* 2017). Conti *et al.* (2013) carried out a pseudo-static analysis of cantilever sheet pile walls using limit equilibrium method by taking the magnitudes of passive earth pressure coefficient as its static value and active earth pressure coefficient as its pseudo-static value due to minor difference in static and pseudo-static coefficients below the dredge level. Conte *et al.* (2017) proposed a simple-to-use method for the design of embedded cantilever retaining walls in static and pseudo-static condition assuming rectilinear net earth pressure diagram and adopting the earth pressure coefficients derived using lower-bound approach of limit analysis by Lancellotta (2012). Due to various constraints in performing experiments in field, numerical analysis has been performed to know the effect of excavation on deflection and bending moment of sheet pile walls. Bahrami *et al.* (2018) performed a finite difference analysis by 3D modelling to assess the effect of penetration depth of a diaphragm wall on wall deflection, axial stress of struts and bending moment and observed that for safety of the excavation, the penetration depth need not to be increased. Chowdhury *et al.* (2013, 2016) used FLAC2D computer program to obtain the design parameters for braced excavation and effect of fines, respectively. Jiang *et al.* (2018) investigated the stress and deformation behavior of anchored sheet pile walls. Madabhushi and Zeng (1998) simulated the gravity quay walls under earthquake loading using finite element based code SWANDYNE and compared the results with centrifuge tests. Qu *et al.* (2016) designed the sheet pile retaining walls through capacity spectrum method for seismic application. Zhang *et al.* (2015, 2019) and Goh *et al.* (2017a, b) carried out assessment of strut forces and deflection of braced excavation wall using numerical analysis and field measurements. Zhang *et al.* (2017) performed inverse analysis of soil and wall properties in braced excavation using multivariate adaptive regression splines. Lee *et al.* (2018) carried out a two dimensional and three dimensional finite element based analysis to check the field applicability of controllable prestressed wale system. Zhang *et al.* (2018)

*Corresponding author, Assistant Professor
E-mail: kchatfce@iitr.ac.in
[a]Research Scholar, Ph.D.
E-mail: asingh4@ce.iitr.ac.in

http://www.techno-press.org/?journal=gae&subpage=7
ISSN: 2005-307X (Print), 2092-6219 (Online)

developed a simple numerical model of braced excavation to investigate the influence of ground water drawdown and soil properties on ground surface settlement. Zhang *et al.* (2018a, b) studied the response of braced excavation in residual soils to groundwater drawdown. Chen *et al.* (2019) performed shaking table test to analyze the characteristics of landslides in granular soil. Goh *et al.* (2019) carried out both deterministic and reliability analysis to study the stability against basal heave of an excavation considering spatial variability in soils. Zhang *et al.* (2020) performed shaking table test to study the response of double box utility tunnel having joint connections under seismic forces.

There are very few available literature showing the influence of external surcharge load on retaining walls, which is a common practice to occur (Steenfelt and Hansen 1984, Motta 1994, Georgiadis and Anagnostopoulos 1998, Caltabiano *et al.* 2012, Singh and Chatterjee 2020c, d). Steenfelt and Hansen (1984) provided complete analytical solution to demonstrate the effect of strip load on the design of sheet pile walls using Brinch Hansen's earth pressure theory. Motta (1994) provided a closed form solution for retaining wall having inclined backfill with surcharge at different distance. Georgiadis and Anagnostopoulos (1998) conducted the model sheet pile wall tests in sand to investigate the effect of surcharge strip loads on wall behaviour. Graphical solutions, combining both elastic and plastic approaches, have been used to determine lateral earth pressure due to external surcharge load.

However, the influence of surcharge load on cantilever sheet pile walls, placed at varying distances, from the top of the wall, under seismic conditions is scarce in literature, and the present study fills up this existing research gap. Though, pseudo-static approach is crude estimate as compared to dynamic nature of earthquake loading, in this method the dynamic effects of earthquake shaking are represented by single, constant horizontal and vertical pseudo-static acceleration coefficients (hence forces) acting through the centroid of the failure mass. Pseudo-static based simulation is generally considered conservative and may compensate possible acceleration amplification. However, pseudo-static approach is generally allowed for non-cohesive soil and earthquakes of representative frequencies less than 5Hz which results in wavelength (>20 m) higher than the retaining wall (Conte *et al.* 2017). Hence, the present study investigates the influence of surcharge load on cantilever sheet pile walls under different pseudo-static conditions using finite difference based computer program FLAC2D (Itasca 2016).

2. Numerical modelling of cantilever sheet pile walls

Numerical modelling of cantilever sheet pile walls (CSPW) with surcharge under pseudo-static condition is carried out in the present study assuming a two-dimensional and plane strain problem using the finite difference based computer program FLAC2D (Itasca 2016). The size of domain and mesh are reserved as per the convergence study as discussed later in the paper. The soil is assumed to be fully dry and saturated, above and below the water table, respectively. The excavation process is simulated in three steps, i.e., wall installation, dewatering and excavation. The excavation is carried in two levels and same construction sequence is followed.

The mesh and the boundary conditions for the present study is shown in Fig. 1. Movement of vertical boundaries are allowed in vertical direction and restrained in horizontal direction. Further, the movement of bottom boundary are restrained in both horizontal and vertical directions. The water table is assumed at 2 m below the ground surface.

An elastic-perfectly plastic Mohr-Coulomb model is used to model the soil, the properties of which are tabulated in Table 1. According to Mohr-Coulomb failure criterion, the failure occurs when the shear stress due to the external loading exceeds the shear strength of the soil in which the sheet pile is embedded. However in the present study, the failure of the CSPW model is considered when the shear stress equals the shear strength, other than at the neighboring zones, of the cantilever sheet pile walls. The soil-wall interface is represented by parameters like soil-wall interface angle (δ), normal stiffness (K_n) and shear stiffness (K_s). The soil-wall interface friction angle is specified to 2/3 of the friction angle of soil. Beam element is used to model the steel sheet pile wall with properties as given in Table 2. According to Itasca (2016), the normal and shear stiffness values are 10 times the equivalent stiffness of the stiffest neighboring zone as given by:

$$K_n = K_s = 10\left(\frac{K + \frac{4}{3}G}{\Delta z_{\min}}\right) \tag{1}$$

where K, G and $\Delta Z_{\min}$ are the bulk modulus, shear modulus and the smallest width of adjoining zone in normal direction to the interface.

The FLAC uses Lagrangian calculation scheme in which incremental displacements are added to the coordinates so that the grid moves and deforms with the material it represents. It incorporates the basic governing equation of a solid body. New displacements and velocities are derived from stresses and forces through the equation of motion. The basic equation of motion used is as follows

$$\rho \frac{\partial \dot{u}_i}{\partial t} = \frac{\partial \sigma_{ij}}{\partial x_j} + \rho g_i \tag{2}$$

where u, ρ, t, x_i, g_i and σ_{ij} are displacement, mass density, time, components of coordinate vector, components of gravitational acceleration (body forces) and components of stress tensor.

Since, formulation in FLAC is dynamic and strain rate is related to the velocity as

$$\dot{e}_{ij} = \frac{1}{2}\left[\frac{\partial \dot{u}_i}{\partial x_j} + \frac{\partial \dot{u}_j}{\partial x_i}\right] \tag{3}$$

where $\dot{e}_{ij}$ and $\dot{u}_i$ are strain-rate components and velocity components respectively.

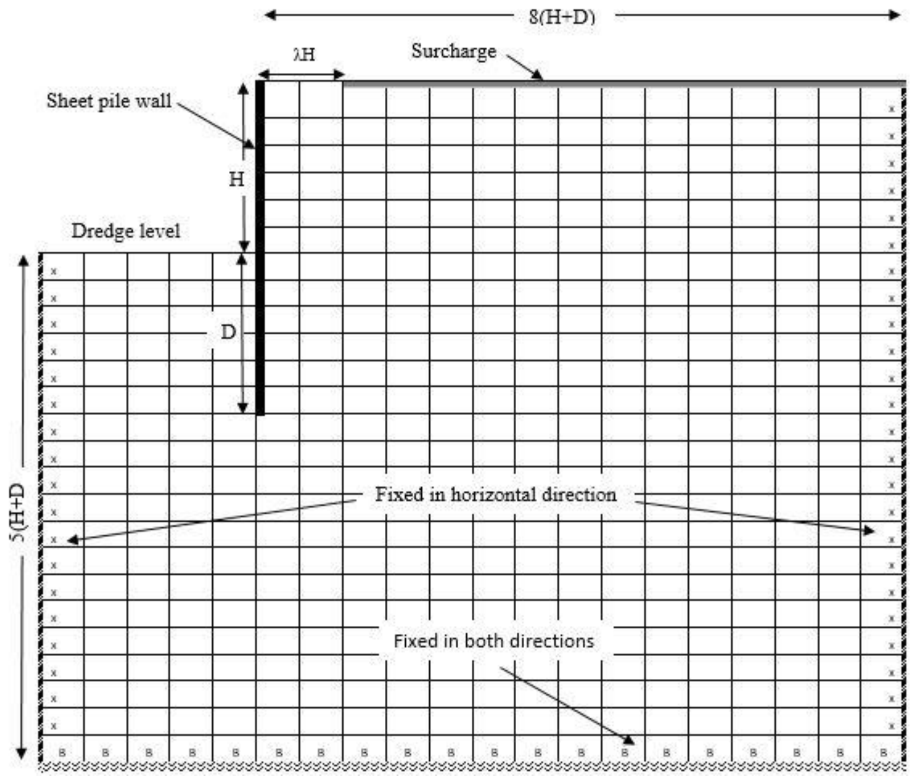

Fig. 1 Cantilever sheet pile wall (CSPW)-soil model considered in the present analysis in FLAC2D

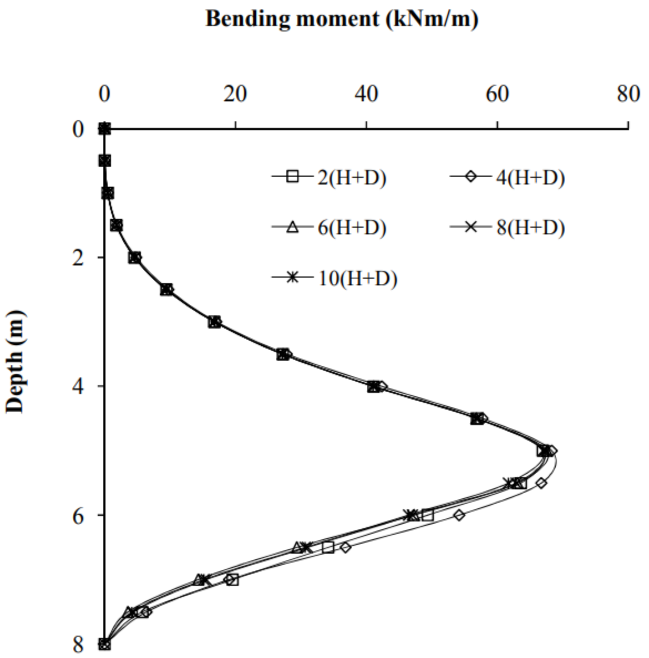

Fig. 2 Variation of bending moment along depth for different width of backfill [mesh size 0.5 m × 0.5 m and depth below dredge level = 5(H+D)]

At a stress boundary, the force can be derived as follows

$$F_i = \sigma_{ij}^{b} n_j \Delta s \tag{4}$$

where n_i is the unit outward normal vector of the boundary segment and Δs is the length of the boundary segment over which the stress σ^b_{ij} acts. The force F_i is added into the force sum for the appropriate gridpoint.

Table 1 Soil properties considered in the present study for pseudo-static analysis of cantilever sheet pile wall (after Chatterjee *et al.* 2015, Bowles 2012)

Soil type	Properties			
	Angle of internal friction (φ)	Poisson's ratio (μ)	Modulus of elasticity (E) in MPa	Unit weight (γ) in kN/m^3
Dense sand	39°	0.30	90	18.4
Medium sand	34°	0.34	65	16.0
Loose sand	30°	0.38	36	14.0

Table 2 Properties of sheet pile walls considered in the present study (adopted from Nucor Skyline 2017)

Type	Cross Section Area (cm^2/m)	Section Modulus (cm^3/m)	Moment of Inertia (cm^4/m)
SKZ 38	234.4	3350	76588

2.1 Convergence study

A numerical analysis is always affected by the boundary conditions, i.e., size of the domain and density of the mesh. Hence, a thorough study to decide the actual size of calculation domain and mesh density is carried out on two-dimensional and plane strain problem having soil properties like unit weight (γ)=20 kN/m^3, soil-friction angle (φ)=35° and interface friction angle (δ)=20° and sheet pile properties such as height of excavation (H)=4 m, depth of embedment (D)=4 m and flexural rigidity (EI)=7.52 x 10^7 kNm^2/m. Fig. 2 shows the variation of bending moment along depth

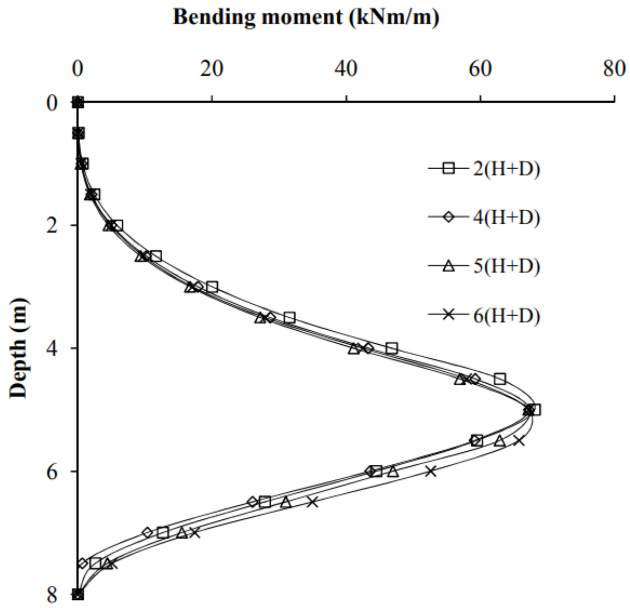

Fig. 3 Variation of bending moment along depth for different depths below dredge level [mesh size 0.5 m × 0.5 m and width of backfill soil = 8(H+D)]

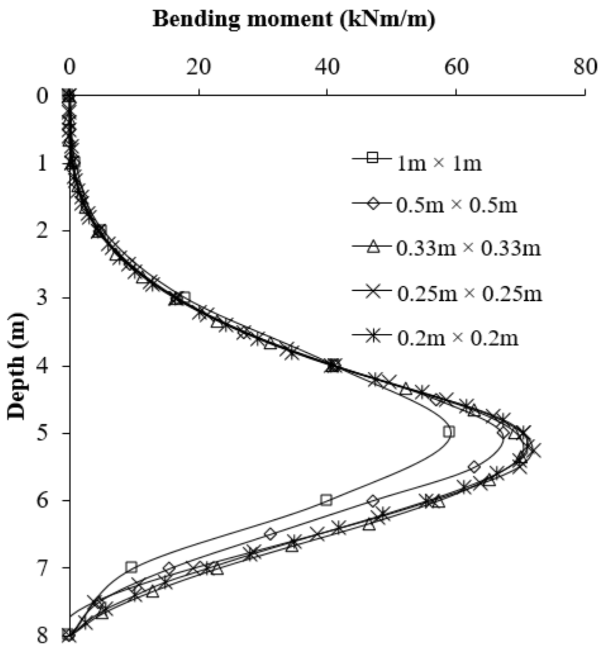

Fig. 4 Variation of bending moment along depth for different mesh sizes [width of backfill soil = 8(H+D) and depth below dredge level = 5(H+D)]

for different width of backfill soil [2(*H*+*D*), 4(*H*+*D*), 6(*H*+*D*), 8(*H*+*D*) and 10(*H*+*D*)] with constant mesh size (0.5 m×0.5 m) and depth below dredge level = 5(*H*+*D*). It is observed that width of backfill soil [6(*H*+*D*), 8(*H*+*D*) and 10(*H*+*D*)] gives approximately the same bending moment along depth. Fig. 3 shows the bending moment versus depth curves for different depths below dredge level [2(*H*+*D*), 4(*H*+*D*), 5(*H*+*D*) and 6(*H*+*D*)] with constant mesh size (0.5 m×0.5 m) and backfill distance = 8(*H*+*D*). It is recognized that for depths below the dredge level [4(*H*+*D*), 5(*H*+*D*) and 6(*H*+*D*)] gives same variation of bending

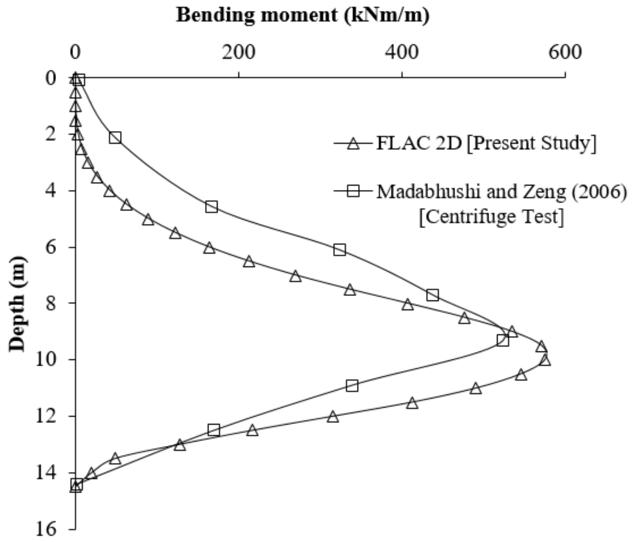

Fig. 5 Comparison of bending moment along depth obtained in the present study without surcharge with that of Madabhushi and Zeng (2006)

moment along depth above the point of maximum bending moment and differs slightly below it. Fig. 4 shows the bending moment versus depth curves for different mesh size with appropriate size of domain selected from Figs. 2 and 3 i.e., backfill distance = 8(*H*+*D*) and depth below dredge level = 5(*H*+*D*). It is observed that mesh size of zones 0.33 m×0.33 m, 0.25 m×0.25 m and 0.2 m×0.2 m gives almost similar trend of bending moment distribution along depths. Hence, it is advocated to select a size of domain having backfill distance = 8(*H*+*D*), depth below dredge level = 5(*H*+*D*) and mesh size of 0.25 m×0.25 m.

2.2 Validation of the present numerical model

The numerical model proposed in the present study, without surcharge load, is validated with the soil properties and input data used by Conti and Viggiani (2013) for simulating the dynamic centrifuge tests carried out by Madabhushi and Zeng (2006). The soil properties considered were unit weight (γ)=16.4 kN/m^3, angle of internal friction (φ)=34º, soil-wall friction angle (δ)=12º and steel sheet pile properties as Young's modulus (E)=68.5 GPa, Poisson's ratio=0.2 at peak acceleration of 0.12g. The excavated depth and embedded depth of the sheet pile were considered was 7.2 m. The depth-wise variation of bending moment in the sheet pile wall is plotted for the present numerical model and the experimental results presented by Conti and Viggiani (2013) as shown in Fig. 5. It is observed that the bending moment distribution of the present numerical model is in good agreement with the results presented by Conti and Viggiani (2013). The discrepancies among the results may be due to implementation of centrifuge test and properties assumed in numerical modeling.

3. Present study

After validation of numerical model, under no surcharge

Table 3 Different input parameters considered in the present study

Parameters	Values
Horizontal seismic acceleration coefficients (k_h)	0, 0.05, 0.1, 0.15 and 0.2
Vertical seismic acceleration coefficients (k_v)	$0k_h$, $0.5k_h$and k_h
Magnitudes of uniform surcharge loading (q)	20 kPa, 50 kPa and 100 kPa
Distance of uniform surcharge load from the top of the wall (λH)	0 m, 1 m, 2 m, 3 m, 4 m, 5 m, 6m, 8 m and 12 m
Height of excavation (H)	4 m
Embedded depths (D)	4 m, 6 m, 8 m and 10 m
Angle of internal friction	φ=30°, φ=34° and φ=39°

loading conditions, the present study is extended to investigate the seismic response of a cantilever sheet pile walls under the influence of surcharge loading and at varying distance from the top of the wall. The results obtained in the present study are presented in non-dimensional form like variation of normalized bending moment and normalized horizontal earth pressures. The various parameters used in the parametric study like embedded depth, type of soil, magnitude and distance of uniform surcharge from the top of the wall at different horizontal and vertical seismic acceleration coefficients are tabulated in Table 3. A cantilever sheet pile wall is considered in homogeneous and isotropic soil layer with height of excavation (H) as 4 m. For all parametric studies, the width of excavation is kept constant as 15 m. Three different types of soils are used in the analysis namely loose sand, medium sand and dense sand with properties as tabulated in Table 1. With various depth of embedment, the magnitude of uniform surcharge and its distance from the top of the wall are varied to study the behavior of sheet pile walls in different type of soils under pseudo-static conditions.

4. Results and discussions

4.1 Influence of seismic acceleration coefficients (k_h and k_v)

The seismic acceleration coefficients under pseudo-static conditions simulate the behavior of earthquake approximately in which earthquake force is applied by a force amplitude constant in direction with time. The effect of seismic acceleration coefficients is analyzed for cantilever sheet pile walls in the form of normalized bending moment and normalized horizontal earth pressure with normalized depth of wall. The variation of normalized maximum bending moment for different seismic acceleration coefficients (k_h and k_v) are given in Table 4. The values of bending moment (M) and horizontal earth pressure are normalized with respect to γH^3 and γH as $M/\gamma H^3$ and $\sigma_h/\gamma H$, respectively and depth is normalized with respect to total length of sheet pile walls and expressed as z/d in percentage. The infinite uniform surcharge is normalized as $q/\gamma H$ and represented as Q. The pattern of normalized bending moment ($M/\gamma H^3$) with normalized depth of wall for horizontal (k_h) as well as vertical (k_v) seismic acceleration coefficients are illustrated in Figs. 6 and 7 respectively. Fig. 6 illustrates the variation of normalized bending moment for k_h=0, 0.05, 0.1, 0.15 and 0.2 at constant k_v=0 while Fig. 7 shows the variation of normalized bending moment for k_v=0, $0.5k_h$ and k_h at constant k_h=0.05 for uniform surcharge Q=0.27 and D/H=2 in dense sand. From Fig. 6, it is observed that the normalized maximum bending moment increases as 0.103, 0.161, 0.208, 0.272 and 0.335 for k_h=0, 0.05, 0.1, 0.15 and 0.2, respectively thus increasing by 279% from static condition to k_h=0.2. Beyond k_h=0.2, the moment is not taken by sheet pile walls due to its failure. Thus, as the horizontal seismic acceleration coefficient is increased, the maximum normalized bending moment also increases following the same pattern of non-dimensional bending moment distribution but the location of maximum non-dimensional bending moment slides down the depth to account the increase of seismic inertia forces. Vertical seismic acceleration coefficients in pseudo-static analysis also destabilizes the sheet pile walls if applied vertically upward which again renders the structure to sustain more bending moment. It is observed from Fig. 7 that keeping k_h=0.05 and increasing k_v from 0, $0.5k_h$ to k_h, the maximum normalized bending moment increases from 0.161,0.179 and 0.191, respectively, thus creating a significant 18% increase in maximum normalized bending moment. From Table 4, it is also seen that beyond k_h=0.1 for k_v=$0.5k_h$ and k_h, the failure of cantilever sheet pile walls takes place.

Table 4 Variation in normalized maximum bending moment for different seismic acceleration coefficients (k_h and k_v), magnitude of surcharge (Q) and normalized embedded depth (D/H)

D/H		$M/\gamma H^3$								
		Q=0.27			Q=0.68			Q=1.36		
	k_v/k_h	0	0.5	1	0	0.5	1	0	0.5	1
	k_h									
1.5	0	0.105	0.105	0.105	0.172	0.172	0.172	0.285	0.285	0.285
	0.05	0.148	0.16	0.174	0.207	0.229	0.241	0.322	0.335	0.338
	0.1	0.199	0.162	0.189	0.245	0.255	0.269	0.333	0.341	0.374
	0.15	0.253	-	-	0.303	-	-	0.362	-	-
	0.2	0.312	-	-	0.340	-	-	0.393	-	-
2	0	0.103	0.103	0.103	0.166	0.166	0.166	0.286	0.286	0.286
	0.05	0.161	0.179	0.191	0.227	0.238	0.257	0.345	0.357	0.368
	0.1	0.208	0.215	0.257	0.252	0.307	0.331	0.358	0.424	0.442
	0.15	0.272	-	-	0.308	-	-	0.378	-	-
	0.2	0.335	-	-	0.365	-	-	0.414	-	-
2.5	0	0.106	0.106	0.106	0.172	0.172	0.172	0.298	0.298	0.298
	0.05	0.176	0.193	0.201	0.234	0.255	0.281	0.359	0.37	0.373
	0.1	0.234	0.240	0.258	0.28	0.3	0.32	0.383	0.442	0.457
	0.15	0.297	-	-	0.34	-	-	0.397	-	-
	0.2	0.360	-	-	0.4	-	-	0.438	-	-

Note: '-' signifies the failure of cantilever sheet pile wall

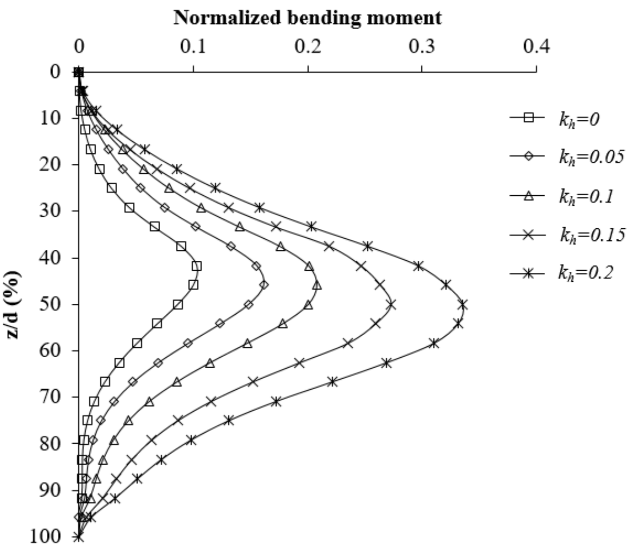

Fig. 6 Variation of normalized bending moment along normalized depth for varying k_h from 0, 0.05, 0.1, 0.15 to 0.2 with k_v=0 and subjected to surcharge load Q=0.27 with D/H=2 in dense sand

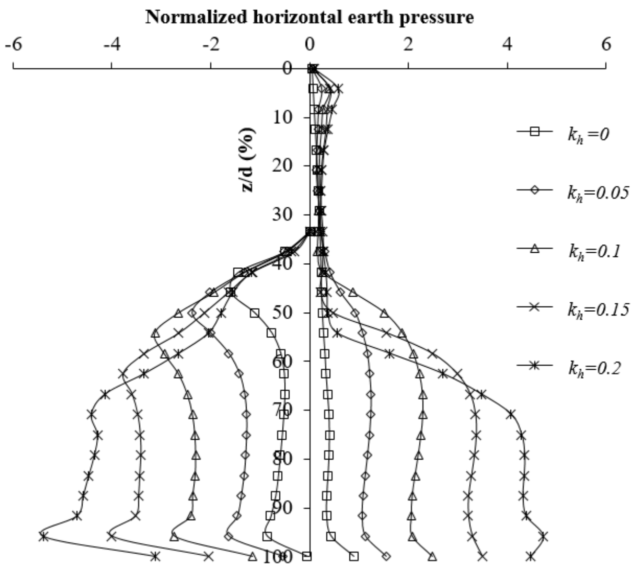

Fig. 8 Variation of normalized horizontal earth pressure with normalized depth for k_h=0, 0.05, 0.1, 0.15 and 0.2, k_v=0k_h at Q=0.27 and D/H=2 in dense sand

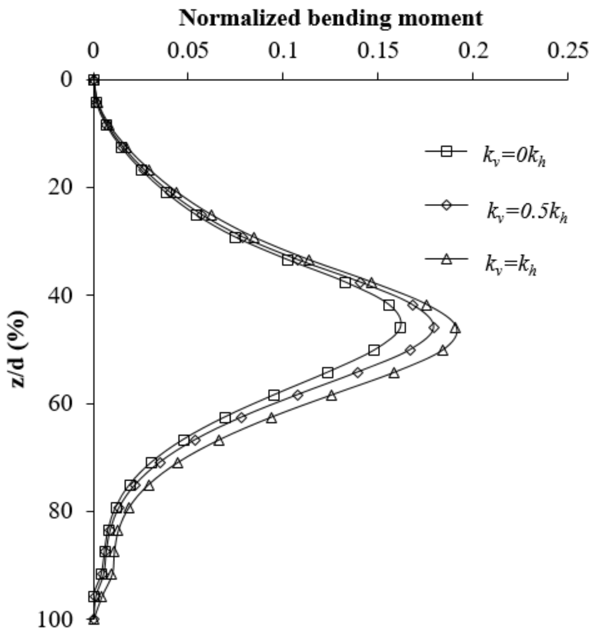

Fig. 7 Variation of normalized bending moment along normalized depth with k_h=0.05 and k_v=0k_h, 0.5k_h to k_h for surcharge load Q=0.27 and D/H=2 in dense sand

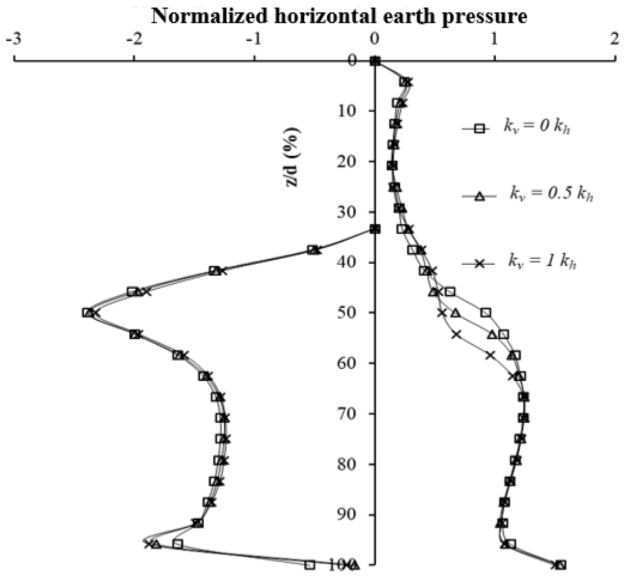

Fig. 9 Variation of normalized horizontal earth pressure with normalized depth for k_v=0k_h, 0.5k_h and k_h with k_h=0.05 at Q=0.27 and D/H=2 in dense sand

Horizontal earth pressures are developed around the sheet pile walls during construction process due to movement of the soil mass. Generally, active earth pressures are fully developed due to wall movement of the order of 0.1% to 0.4% while 5% to 20% wall movement is necessary for full mobilization of passive earth pressure (Bowles 2012). The percentage variation mainly depends on the type of wall movements and soil present in the backfill. Due to less requirement of movement for active earth pressure to be developed, the soil behind the sheet pile walls is in active limit condition up to a certain depth below dredge level, whereas in front of the wall immediately below dredge level, passive earth resistance is fully mobilized. Figs. 8 and 9 illustrate the normalized horizontal earth pressure along normalized depth for k_h=0, 0.05, 0.1, 0.15 and 0.2 with k_v=0 and constant k_h=0.05 and k_v=0, 0.5k_h and k_h with uniform surcharge load Q=0.27 and D/H=2 in dense sand, respectively. It is observed from Fig. 8 that when k_h increases, the active earth pressures in the backfill increase and this increase in the active earth pressure causes mobilization of passive earth resistance to a larger depth to satisfy moment equilibrium in front of the wall. The inertia force in the form of seismic condition redistributes the earth pressure causing increase in bending moment of the sheet pile walls. As active earth pressures are fully developed at less movement of the wall, it can be seen

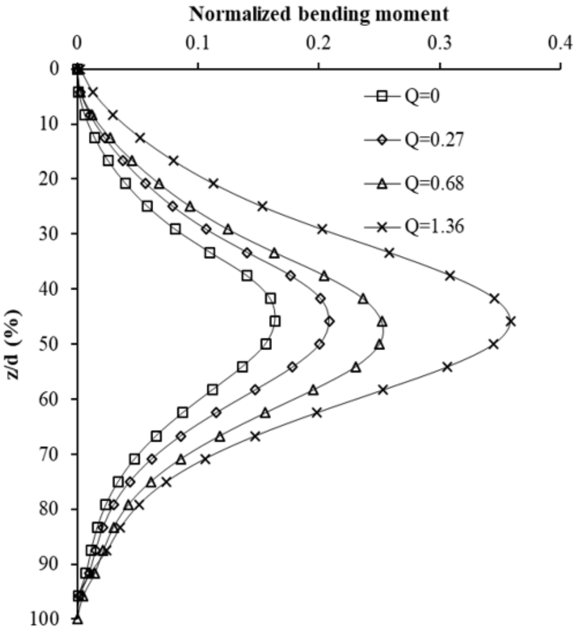

Fig. 10 Variation of normalized bending moment along normalized depth for k_h=0.1, k_v=0k_h and D/H=2 in dense sand for different magnitudes of normalized uniform surcharge load

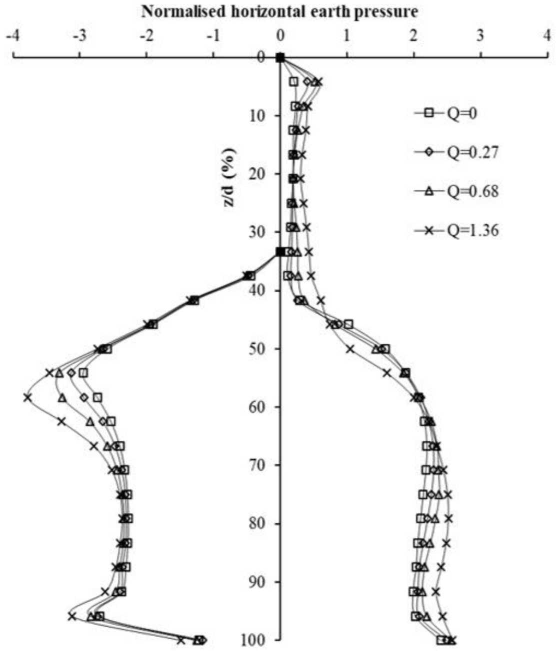

Fig. 12 Variation of normalized horizontal earth pressure along normalized depth for different uniform surcharge Q=0, 0.27, 0.68, 1.36 located at the top of the wall for k_h=0.1, k_v=0k_h with D/H=2 in dense sand

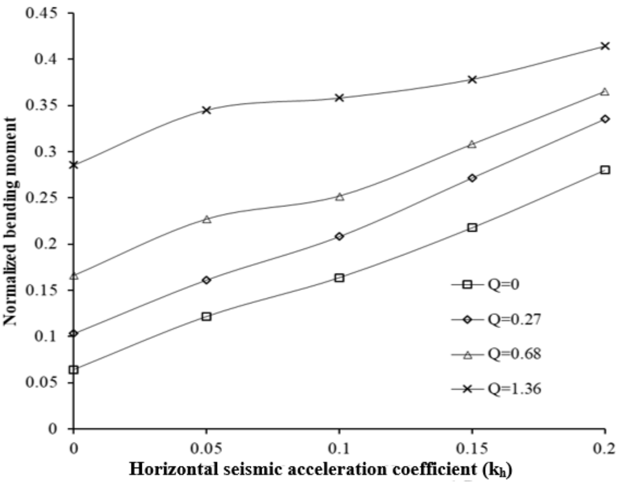

Fig. 11 Variation of normalized bending moment with different k_h, k_v=0k_h for various magnitudes of uniform surcharge at D/H=2 in dense sand

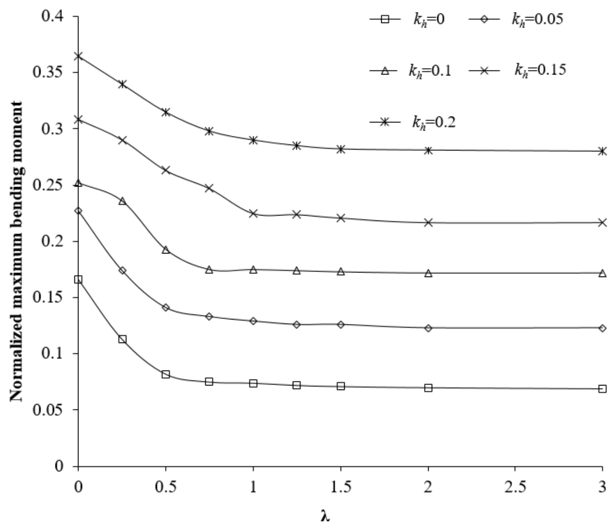

Fig. 13 Variation of normalized maximum bending moment with the normalized distance of uniform surcharge load (λ) for different k_h, k_v=0k_h at Q=0.68 and D/H=2 in dense sand

from Fig. 9 that as k_v increases, the earth pressure profile tends to more mobilization of active earth pressure, resulting in increase in the depth of full mobilization. The influence of horizontal seismic acceleration coefficient on analysis of sheet pile walls is observed more than vertical seismic acceleration coefficient because gravity can counter act the vertical seismic acceleration coefficient but in horizontal direction more unbalanced inertia force are generated due to horizontal seismic acceleration coefficient.

4.2 Influence of magnitude of surcharge load located at the top of the wall

Presence of uniform surcharge load at top of the wall affects the bending moment and horizontal earth pressure by mobilizing the earth pressures. Cantilever sheet pile walls loaded with uniform surcharge at the top of the wall with different normalized embedded depth shows the increase in normalized bending moment with increase in surcharge load as tabulated in Table 4. The magnitude of uniform surcharge (Q) considered in the present study are 0.27, 0.68 and 1.36. Fig. 10 shows the bending moment pattern for different magnitude of surcharge in the form of normalized bending moment along normalized depth for k_h=0.1, k_v=0 and D/H=2 in dense sand. The normalized bending moment increases by 27.2%, 53.8% and 118.7%

from no surcharge case to Q=0.27, 0.68 and 1.36 respectively. It is observed that the maximum bending moment increases with the increase in magnitude of uniform surcharge. It is also observed from Fig. 11 that for all magnitudes of uniform surcharge, the normalized bending moment increases with increase in the horizontal seismic acceleration coefficients. However, the rate of increase of normalized bending moment is dropped with increase in seismic acceleration coefficient at high magnitude of surcharge. The drop may be due to the application of high inertia force.

Fig. 12 illustrates the effect of surcharge load on normalized horizontal earth pressure along the normalized depth of wall for different magnitudes of uniform surcharge for k_h=0.1, k_v=0 with *D/H*=2 in dense sand. It is observed that as the surcharge load is increased from no surcharge condition (*Q*=0) to different magnitudes of uniform surcharge (*Q*=0.27, 0.68 and 1.36), the lateral earth pressures around the wall increases, thus increasing the depth of full mobilization of passive earth resistance below the dredge level. This increase in the earth pressure increases the bending moment to satisfy moment equilibrium condition as shown in Figs. 10 and 11. It is also observed that patterns of earth pressure are similar for different magnitudes of uniform surcharge.

4.3 Influence of position of uniform surcharge (λ)

The existence of surcharge at a distance from the top of the wall on the backfill soil is a normal condition that may occur at any point of time during the life of a structure. Although, these structures apply load on the bounded space, but in the present study it is assumed to be acting as an infinite uniform surcharge. The uniform surcharge loading is placed at various distances from top of the wall (*b*=1 m, 2 m, 3 m, 4 m, 5 m, 6 m, 8 m and 12 m). The position of surcharge at a distance from the top of the wall is accounted using a normalized parameter λ, defined as, the ratio of distance of uniform surcharge from the top of the wall to height of excavation (*H*). The variation in normalized bending moment for different normalized distances from the top of the wall, magnitudes of uniform surcharge and horizontal seismic acceleration coefficients are tabulated in Table 5. The effect of uniform surcharge (*Q*=0.68) at a normalized distance from the top of the wall (λ) is investigated with respect to normalized maximum bending moment and normalized horizontal earth pressure for k_h=0, 0.05, 0.1, 0.15 and 0.2 as shown in Fig. 13 and for different magnitude of surcharge as shown in Fig. 14. It is observed from Fig. 13 that for k_h=0.1 and k_v=0, the normalized maximum bending moment varies as 0.252, 0.236, 0.193, 0.175, 0.175, 0.174, 0.173, 0.172 and 0.172 for normalized distance of surcharge (λ) as 0, 0.25, 0.5, 0.75, 1, 1.25, 1.5, 2 and 3, respectively. The decrement of about 32 % is observed between the position of surcharge at top of the wall and far away (λ=3) from the top of the wall. It is also observed that for different values of k_h, if the distance of uniform surcharge increases from the top of the wall, the normalized maximum bending moment decreases to a certain value and remains almost constant after λ=1. The constant value of normalized maximum bending moment is approximately the same which occurs at no surcharge condition for all values of k_h.

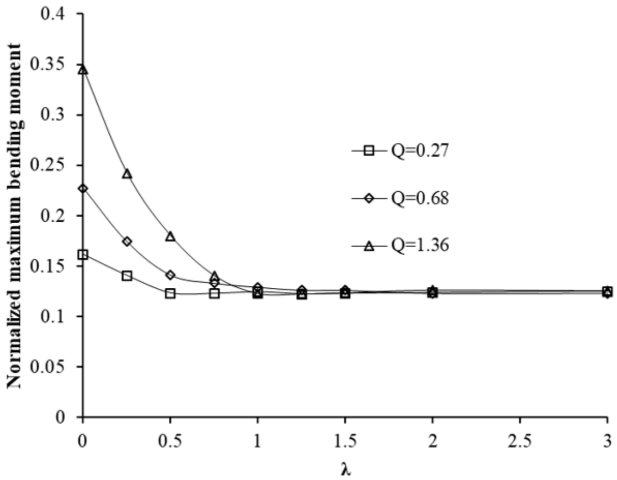

Fig. 14 Variation of normalized maximum bending moment with the normalized distance of uniform surcharge for different magnitude of uniform surcharge at k_h=0.05, k_v=0k_h and *D/H*=2 in dense sand

Table 5 Variation in normalized bending moment for different λ, k_h and q at k_v=0k_h, *D/H*=2 in dense sand

Q	k_h	$M/\gamma H^3$								
		λ								
		0	0.25	0.5	0.75	1	1.25	1.5	2	3
0.27	0	0.103	0.081	0.069	0.067	0.067	0.066	0.066	0.065	0.065
	0.05	0.161	0.140	0.130	0.123	0.123	0.122	0.121	0.119	0.119
	0.1	0.208	0.188	0.187	0.183	0.178	0.173	0.165	0.165	0.160
	0.15	0.291	0.273	0.242	0.238	0.225	0.222	0.222	0.221	0.217
	0.2	0.335	0.311	0.294	0.288	0.281	0.278	0.273	0.272	0.267
0.68	0	0.166	0.113	0.082	0.075	0.074	0.072	0.071	0.070	0.069
	0.05	0.227	0.174	0.141	0.133	0.129	0.126	0.126	0.123	0.123
	0.1	0.252	0.236	0.193	0.175	0.175	0.174	0.173	0.172	0.172
	0.15	0.308	0.290	0.263	0.247	0.225	0.224	0.221	0.217	0.217
	0.2	0.365	0.340	0.315	0.298	0.290	0.285	0.282	0.281	0.280
1.36	0	0.286	0.193	0.125	0.084	0.080	0.075	0.074	0.074	0.072
	0.05	0.330	0.242	0.180	0.141	0.130	0.128	0.127	0.126	0.125
	0.1	0.358	0.285	0.243	0.197	0.181	0.179	0.178	0.178	0.174
	0.15	0.378	0.363	0.292	0.258	0.240	0.221	0.220	0.219	0.219
	0.2	0.414	0.396	0.361	0.342	0.330	0.310	0.302	0.302	0.301

Fig. 14 shows the variation of normalized maximum bending moment with respect to normalized distance of surcharge from the top of the wall (λ) for different magnitudes of surcharge (*Q*=0.27, 0.68 and 1.36). For uniform surcharge of 0.68 and k_h=0.05 and k_v=0, the normalized maximum bending moment varies as 0.227, 0.174, 0.141, 0.133, 0.129, 0.126, 0.126, 0.123 and 0.123 for normalized distance of surcharge (λ) as 0, 0.25, 0.5, 0.75, 1, 1.25, 1.5, 2 and 3, respectively. The maximum decrement of about 46% is observed between the position of surcharge at top of the wall and far away from top of the

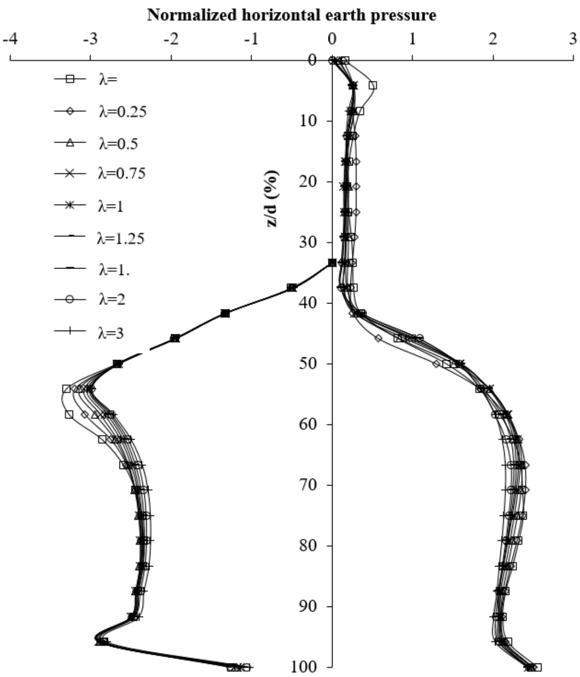

Fig. 15 Variation of normalized horizontal earth pressure with normalized depth for different normalized distance of uniform surcharge from the top of the wall at Q=0.68 and k_h=0.1, k_v=0k_h with D/H=2 in dense sand

wall. Similar decrement in normalized maximum bending moment are also observed in case of Q=0.27 and Q=1.36 by 22.4% and 63%, respectively as tabulated in Table 5. It is clearly observed from Table 5 that normalized bending moment decreases with increase in distance of surcharge from the top of the wall and with increase in magnitude of surcharge, it increases. This means that the magnitude of uniform surcharge does not affect the structure beyond a certain distance and the structure behaves like a no surcharge condition but as the magnitude of surcharge increases, the effect is experienced up to a larger distance than less magnitude of surcharge.

Fig. 15 shows the variation of normalized horizontal earth pressure along the normalized depth of wall for different positions of surcharge having normalized magnitude 0.68 at k_h=0.1, k_v=0 with D/H=2 in dense sand. It is observed that maximum lateral earth pressure around the cantilever sheet pile wall are obtained in the case when the surcharge is at top of the wall. As the position of surcharge is changed from top of the wall (λ=0) to a normalized distance λ=3, the lateral earth pressures decrease to a value corresponding to a condition where there is no surcharge load on the cantilever sheet pile wall.

4.4 Influence of angle of internal friction

Behavior of any geotechnical structure changes with the type of soil because mobilization of active and passive earth pressure depends on type of soil in which structure is present. Figs. 16 and 17 show the variation of normalized maximum bending moment with varying k_h and k_v=0 for different angle of internal friction with D/H=2. It is observed from Fig. 16 that as the k_h changes from 0, 0.05,

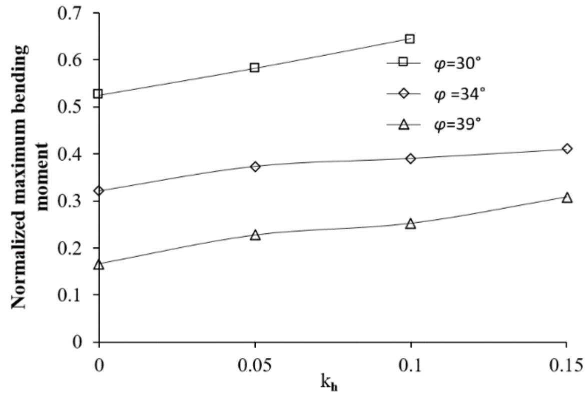

Fig. 16 Variation of normalized maximum bending moment with k_h=0, 0.05, 0.1 and 0.15, k_v=0$k_h$for different angle of internal friction of soil (φ) at q=50 kPa, D/H=2

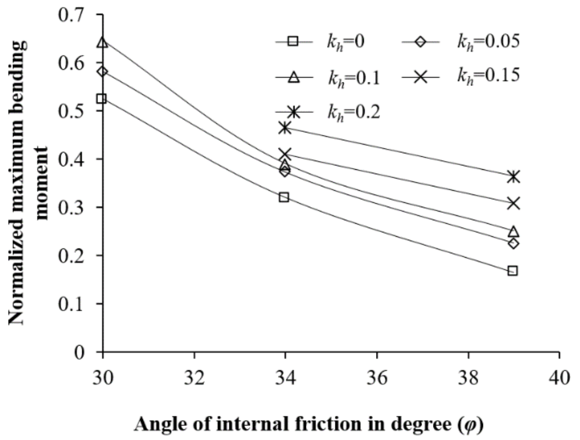

Fig. 17 Variation of normalized maximum bending moment with different angle of internal friction of soil (φ) for different k_h, k_v=0k_h at q=50 kPa, D/H=2

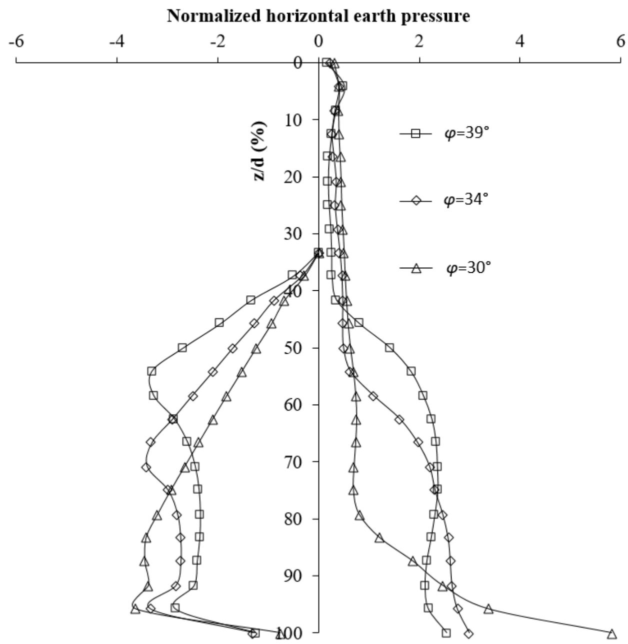

Fig. 18 Variation of normalized horizontal earth pressure with normalized depth for different angle of internal friction at k_h=0.1, k_v=0k_h, q= 50 kPa at the top of the wall (λ=0) and D/H=2

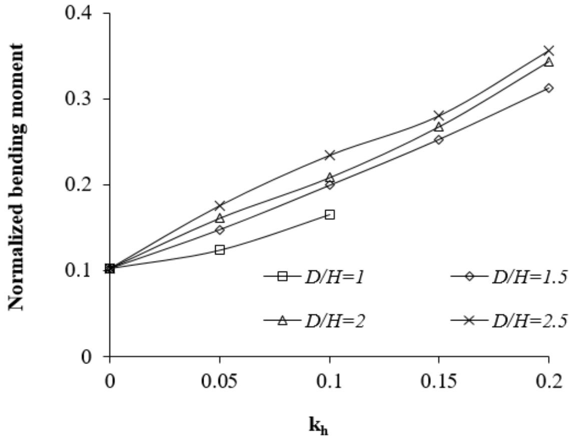

Fig. 19 Variation of normalized maximum bending moment with k_h for different D/H at k_v=0k_h, Q=0.27 in dense sand

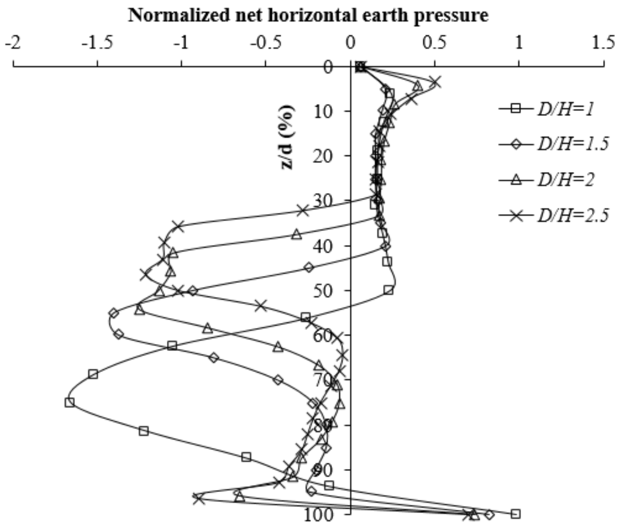

Fig. 20 Variation of normalized net horizontal earth pressure along normalized depth for different normalized embedded depth (D/H) at k_h=0.1, k_v=0k_h and Q=0.27 in dense sand

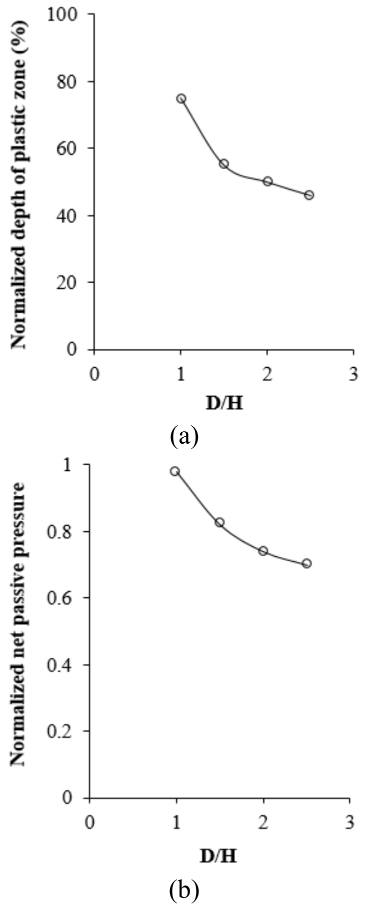

Fig. 21 Effect of the normalized embedded depth (D/H) on (a) normalized depth of full mobilization of passive earth resistance below dredge level and (b) normalized net pressure at the wall toe

0.1 to 0.15, the normalized maximum bending moment increases as 0.32, 0.37, 0.39 and 0.41, respectively for φ=34°. A similar trend is also observed for both φ=30° and φ=39°. From Fig. 17, it is observed that as the denseness increases corresponding to increase in angle of internal friction, for a particular seismic acceleration coefficient, the normalized maximum bending moment decreases. Also, at higher seismic conditions, i.e., k_h=0.15 and 0.2, the cantilever sheet pile walls could not sustain higher bending moments for φ=30° and hence gets failed.

Fig. 18 illustrates the normalized horizontal earth pressure with normalized depth for φ=30°, φ=34° and φ=39°. It is observed that for k_h=0.1, k_v=0, λ=0 and q=50kPa with D/H=2 at φ=39°, the earth pressure in case of φ=30° gets mobilized to a greater depth than φ=34° and φ=39°. The greater mobilization in case of φ=30° is attributed to less resistance offered by the soil particles owing to lower angle of internal friction as compared to φ=34° and φ=39°.Also, the active earth pressure in φ=30° is more than φ=34° and φ=39° due to less angle of internal friction, thus creating more earth thrust and hence more bending moments.

4.5 Influence of embedded depth (D)

Cantilever sheet pile wall generally derives its stability from the passive earth resistance developed below the dredge level. So, the effect of horizontal seismic acceleration coefficients on normalized maximum bending moment and earth pressure of cantilever sheet pile walls for various normalized embedded depths (D/H) and uniform surcharge are summarized in Table 4.

It is observed from Fig. 19 that with an increase in k_h, the maximum normalized bending moment also increases for different normalized embedded depth. The normalized maximum bending moment increases as 0.165, 0.2, 0.208 and 0.234 with D/H as 1, 1.5, 2 and 2.5, respectively for k_h=0.1, k_v=0 under surcharge load of 0.27 in dense sand. It is because as the embedded depth increases, the sheet pile walls become more stable and sustains more load and hence more bending moment. It is also observed that if the embedded depth is small, the structure cannot sustain high seismic condition as seen for D/H=1 due to less availability of embedded depth. Fig. 20 shows the variation of normalized net earth pressure along normalized depth (*z/d*) for various normalized embedded depths (*D/H*) to show the development of plastic zone below dredge level. The plastic zone is defined as the zone up to which full mobilization of passive earth resistance below the dredge level exists. It is observed that as the normalized embedded depth increases, the development of plastic zone and net passive pressure at bottom of the wall decreases. The variation of decrease of depth of plastic zone as well as net earth pressure at toe of the wall with different normalized embedded depths are given in Fig. 21. It is observed from Fig. 21 that as the embedded depth increases, the development of plastic zone below the dredge level and net earth pressure at toe of the wall decreases. This decrement in development of plastic zone below the dredge level and net earth pressure at toe of the wall occurs due to significant reduction of the horizontal displacement of the sheet pile walls. A similar pattern of development of plastic zone below the dredge level and net earth pressure at toe of the wall was observed by Conte *et al.* (2017) for cantilever sheet pile walls under no surcharge loading conditions.

5. Conclusions

Pseudo-static analysis of cantilever sheet pile walls with varying distance of different surcharge from the top of the wall in three different soil conditions is carried out in the present study by using the finite difference based computer program FLAC2D. The numerical model without surcharge loading is validated with the existing experimental as well as analytical results and extended to study the influence of surcharge loading on cantilever sheet pile walls under seismic conditions. The major conclusions drawn from the present study are:

• The horizontal earth pressures and bending moment of cantilever sheet pile walls under surcharge loading are influenced by many factors like embedded depth, distance of surcharge from the top of the wall, seismic acceleration coefficients and type of soil.

• The inertia forces in the form of seismic acceleration coefficient increases the maximum bending moment and mobilization of earth pressure. The horizontal seismic acceleration coefficients affect the cantilever sheet pile walls more than the vertical seismic acceleration coefficients. The increase in normalized bending moment is 279% from static condition to k_h=0.2 (k_v=0) and 18% when k_v=k_h (k_h=0.05) in dense sand as backfill soil subjected to 0.27 uniform surcharge load and *D/H*=2.

• According to the results, the presence of surcharge develops more lateral earth pressure resulting in an increase in bending moment to satisfy the moment equilibrium condition. The effect is more when the surcharge is at the top of the wall and gets reduced beyond a certain distance, i.e., λ=1 to no surcharge condition on seismic response of cantilever sheet pile walls.

• The behavior of cantilever sheet pile walls changes with angle of internal friction. The soil with φ=39° being stiffer is less mobilized along the depth of the wall than φ=34° and φ=30° for same seismic conditions. Hence, the bending moment is observed to increase with increase in angle of internal friction.

• The depth of embedment has significant effects on the behavior of cantilever sheet pile walls. The stability of the wall increases with increase in depth of embedment in seismic condition. At low depth of embedment i.e., *D/H*=1, k_h is limited to 0.1 while for others k_h is up to 0.2. Also, the normalized depth of plastic zone and net passive earth pressure at toe of the wall decreases as the embedded depth increases.

Therefore, the finite difference method can be used for safe design of cantilever sheet pile walls with surcharge at the top of the wall during seismic condition. Moreover, in the present study the influence of surcharge at varying distance on the backfill is considered, which has not been addressed by previous researchers. However, the results obtained in the present study are valid in certain conditions in which it is carried out. Hence, the present study might be of interest to site engineers for safe design of cantilever sheet pile walls adjacent to uniform surcharge in seismic conditions.

References

Bahrami, M., Khodakarami, M.I. and Haddad, A. (2018), "3D numerical investigation of the effect of wall penetration depth on excavations behavior in sand", *Comput. Geotech.*, **98**, 82-92. https://doi.org/10.1016/j.compgeo.2018.02.009.

Bowles, J.E. (2012), *Foundation Analysis and Design*, 5th Edition, McGraw Hill, New York.

Callisto, L. (2014), "Capacity design of embedded retaining structures", *Géotechnique*, **64**(3), 204-214. https://doi.org/10.1680/geot.13.P.091.

Callisto, L. and Soccodato, F.M. (2010), "Seismic design of flexible cantilevered retaining walls", *J. Geotech. Geoenviron. Eng.*, **136**(2), 344-354. https://doi.org/10.1061/(ASCE)GT.1943-5606.0000216.

Caltabiano, S., Cascone, E. and Maugeri, M. (2012), "Static and seismic limit equilibrium analysis of sliding retaining walls under different surcharge conditions", *Soil Dyn. Earthq. Eng.*, **37**, 38-55. https://doi.org/10.1016/j.soildyn.2012.01.015.

Chatterjee, K., Choudhury, D. and Poulos, H.G. (2015), "Seismic analysis of laterally loaded pile under influence of vertical loading using finite element method", *Comput. Geotech.*, **67**, 172-186. https://doi.org/10.1016/j.compgeo.2015.03.004.

Chen, Z., Yang, P., Liu, H., Zhang, W. and Wu, C. (2019), "Characteristics analysis of granular landslide using shaking table model test", *Soil Dyn. Earthq. Eng.*, **126**, 105761. https://doi.org/10.1016/j.soildyn.2019.105761.

Chowdhury, S.S., Deb, K. and Sengupta, A. (2016), "Effect of fines on behavior of braced excavation in sand: Experimental and numerical study", *Int. J. Geomech.*, **16**(1), 04015018. https://doi.org/10.1061/(ASCE)GM.1943-5622.0000487.

Chowdhury, S.S., Deb, K. and Sengupta, A. (2013), "Estimation of design parameters for braced excavation: A numerical study", *Int. J. Geomech.*, **13**(3), 234-247. https://doi.org/10.1061/(ASCE)GM.1943-5622.0000207.

Conte, E., Troncone, A. and Vena, M. (2017), "A method for the design of embedded cantilever retaining walls under static and seismic loading", *Géotechnique*, **67**(12), 1081-1089. https://doi.org/10.1680/jgeot.16.P.201.

Conti, R., Viggiani, G.M.B. and Buralid'Arezzo, F. (2014), "Some remarks on the seismic behaviour of embedded cantilevered retaining walls", *Géotechnique*, **64**(1), 40-50. https://doi.org/10.1680/geot.13.P.031.

Conti, R., De Sanctis, L. and Viggiani, G.M.B. (2012), “Numerical modelling of installation effects for diaphragm walls in sand”, *Acta Geotechnica*, **7**(3), 219-237. https://doi.org/10.1007/s11440-011-0157-0.

Conti. R. and Viggiani. G.M.B. (2013), “A new limit equilibrium method for the pseudostatic design of embedded cantilevered retaining walls”, *Soil Dyn. Earthq. Eng.*, **50**, 143-150. https://doi.org/10.1016/j.soildyn.2013.03.008.

Georgiadis, M. and Anagnostopoulos, C. (1998), “Lateral pressure on sheet pile walls due to strip load”, *J. Geotech. Geoenviron. Eng.*, **124**(1), 95-98. https://doi.org/10.1061/(ASCE)1090-0241(1998)124:1(95).

Goh, A.T.C., Zhang, F., Zhang, W. and Chew, O.Y.S. (2017a), “Assessment of strut forces for braced excavation in clays from numerical analysis and field measurements”, *Comput. Geotech.*, **86**, 141-149. https://doi.org/10.1016/j.compgeo.2017.01.012.

Goh, A.T.C., Zhang, F., Zhang, W., Zhang, Y. and Liu, H. (2017b), “A simple estimation model for 3D braced excavation wall deflection”, *Comput. Geotech.*, **83**, 106-113. https://doi.org/10.1016/j.compgeo.2016.10.022.

Goh, A.T.C., Zhang, W.G. and Wong, K.S. (2019), “Deterministic and reliability analysis of basal heave stability for excavation in spatial variable soils”, *Comput. Geotech.*, **108**, 152-160. https://doi.org/10.1016/j.compgeo.2018.12.015.

Itasca (2016), *User’s Guide for FLAC2D*, Version 8.0, Itasca Consulting Group, Minneapolis, Minnesota, U.S.A.

Jiang, S., Du, C. and Sun, L. (2018), “Numerical analysis of sheet pile wall structure considering soil-structure interaction”, *Geomech. Eng.*, **16**(3), 309-320. https://doi.org/10.12989/gae.2018.16.3.309.

King, G.J.W. (1995), “Analysis of cantilever sheet-pile walls in cohesionless soil”, *J. Geotech. Eng.*, **121**(9), 629-635. https://doi.org/10.1061/(ASCE)0733-9410(1995)121:9(629).

Lancellotta, R. (2012), *Geotecnica*, 4th Edition, Zanichelli, Bologna, Italy.

Lee, C.I., Kim, E.K., Park, J.S. and Lee, Y.J. (2018), “Preliminary numerical analysis of controllable prestressed wale system for deep excavation”, *Geomech. Eng.*, **15**(5), 1061-1070. https://doi.org/10.12989/gae.2018.15.5.1061.

Madabhushi, S.P.G. and Chandrasekaran, V.S. (2005), “Rotation of cantilever sheet pile walls”, *J. Geotech. Geoenviron. Eng.*, **131**(2), 202-212. https://doi.org/10.1061/(ASCE)1090-0241(2005)131:2(202).

Madabhushi, S.P.G. and Zeng, X. (1998), “Seismic response of gravity quay walls. II: numerical modelling”, *J. Geotech. Geoenviron. Eng.*, **124**(5), 418-427. https://doi.org/10.1061/(ASCE)1090-0241(1998)124:5(418).

Madabhushi, S.P.G. and Zeng, X. (2006), “Seismic response of flexible cantilever retaining walls with dry backfill”, *Geomech. Geoeng.*, **1**(4), 275–-289. https://doi.org/10.1080/17486020601039170.

Motta, E. (1994) “Generalized Coulomb active-earth pressure for distanced surcharge”, *J. Geotech. Eng.*, **120**(6), 1072-1079. https://doi.org/10.1061/(ASCE)0733-9410(1994)120:6(1072).

Nucor Skyline (2017), Technical Product Manual, New Jersey, USA. https://www.nucorskyline.com.

Qu, H., Li, R., Hu, H., Jia, H. and Zhang, J. (2016), “An approach of seismic design for sheet pile retaining wall based on capacity spectrum method”, *Geomech. Eng.*, **11**(2), 309-323. https://doi.org/10.12989/gae.2016.11.2.309.

Singh, A.P. and Chatterjee, K. (2020a), “A simplified method for seismic design of cantilever sheet pile walls under infinite uniform surcharge load”, *Int. J. Geomech.*, **20**(9), 04020139-1_04020139-11. https://doi.org/10.1061/(ASCE)GM.1943-5622.0001764.

Singh, A.P. and Chatterjee, K. (2020b), “Effect of soil-wall friction angle on behaviour of sheet pile wall under surcharge loading”, *Proc. Nat. Acad. Sci. India Section A Phys. Sci.* https://doi.org/10.1007/s40010-020-00657-1.

Singh, A.P. and Chatterjee, K. (2020c), “Ground settlement and deflection response of cantilever sheet pile wall subjected to surcharge”, *Indian Geotech. J.*, **50**(4), 540-549. https://doi.org/10.1007/s40098-019-00387-1.

Singh, A.P. and Chatterjee, K. (2020d), “Influence of soil type on static response of cantilever sheet pile walls under surcharge loading: A numerical study”, *Arab. J. Geosci.*, **13**(3), 138. https://doi.org/10.1007/s12517-020-5170-x.

Steenfelt, J.S. and Hansen, B. (1984), “Sheet pile design earth pressure for strip load”, *J. Geotech. Eng.*, **110**(7), 976-986. https://doi.org/10.1061/(ASCE)0733-9410(1984)110:7(976).

Zhang, R., Zhang, W., Goh, A.T.C., Hou, Z. and Wang, W. (2018), “A simple model for ground surface settlement induced by braced excavation subjected to a significant groundwater drawdown”, *Geomech. Eng.*, **16**(6), 635-642. https://doi.org/10.12989/gae.2018.16.6.635.

Zhang, W.G., Goh, A.T.C., Goh, K.H., Chew, O.Y.S., Zhou, D. and Zhang, R. (2018a), “Performance of braced excavation in residual soil with groundwater drawdown”, *Undergr. Sp.*, **3**(2), 150-165. https://doi.org/10.1016/j.undsp.2018.03.002.

Zhang, W., Wang, W., Zhou, D., Zhang, R., Goh, A.T.C. and Hou, Z. (2018b), “Influence of groundwater drawdown on excavation responses–A case history in Bukit Timah granitic residual soils”, *J. Rock Mech. Geotech. Eng.*, **10**(5), 856-864. https://doi.org/10.1016/j.jrmge.2018.04.006.

Zhang, W., Goh, A.T.C. and Xuan, F. (2015), “A simple prediction model for wall deflection caused by braced excavation in clays”, *Comput. Geotech.*, **63**, 67-72. https://doi.org/10.1016/j.compgeo.2014.09.001.

Zhang, W., Han, L., Feng, L., Ding, X., Wang, L., Chen, Z., Liu, H., Aljarmouzi, A. and Sun, W. (2020), “Study on seismic behaviors of a double box utility tunnel with joint connections using shaking table model tests”, *Soil Dyn. Earthq. Eng.*, **136**, 106118. https://doi.org/10.1016/j.soildyn.2020.106118.

Zhang, W., Hou, Z., Goh, A.T.C. and Zhang, R. (2019), “Estimation of strut forces for braced excavation in granular soils from numerical analysis and case histories”, *Comput. Geotech.*, **106**, 286-295. https://doi.org/10.1016/j.compgeo.2018.11.006.

Zhang, W., Zhang, Y. and Goh, A.T.C. (2017), “Multivariate adaptive regression splines for inverse analysis of soil and wall properties in braced excavation”, *Tunn. Undergr. Sp. Tech.*, **64**, 24-33. https://doi.org/10.1016/j.tust.2017.01.009.

CC

List of symbols

D	embedded depth
d	total length of cantilever sheet pile walls
E	modulus of elasticity
EI	flexural rigidity
G	shear modulus
H	height of excavation
I	moment of inertia

K	bulk modulus
k_a	coefficient of active earth pressure
k_h	horizontal seismic acceleration coefficient
K_n	normal stiffness
k_p	coefficient of passive earth pressure
K_s	shear stiffness
k_v	vertical seismic acceleration coefficient
M	bending moment
Q	normalized magnitude of infinite uniform surcharge
q	uniform surcharge
z	depth measured below ground level
γ	unit weight of soil
δ	soil-wall interface friction angle
ΔZ_{min}	smallest width of adjoining zone in normal direction to the interface
λ	normalized distance of the surcharge from the top of the wall
μ	Poisson's ratio
σ_h	horizontal earth pressure
φ	soil friction angle